LAWRENCE
LIVERMORE
NATIONAL
LABORATORY

LLNL-JRNL-774812

Surface Complexation Model of Rare Earth Adsorption onto Bacterial Surface with Lanthanide Binding Tags

E. Chang, A. Brewer, D. Park, Y. Jiao, L. Lammers

May 20, 2019

Applied Geochemistry

Disclaimer

Surface Complexation Model of Rare Earth Element Adsorption onto Bacterial Surfaces with Lanthanide Binding Tags

For submission to *Applied Geochemistry*

Elliot Chang[†], Aaron W. Brewer[‡], Dan M. Park[‡], Yongqin Jiao[‡], and Laura N. Lammers[†*]

[†]Department of Environmental Science, Policy, and Management, University of California – Berkeley, Berkeley, California 94709, United States

[‡]Physical and Life Science Directorate, Lawrence Livermore National Laboratory, Livermore, California 92550, United States

* corresponding author: Laura Nielsen Lammers, lnlammers@berkeley.edu

Keywords: surface complexation modeling, rare earth elements, REE, biosorption, bioadsorption, surface complexation, lanthanide binding tag

Abstract

Lanthanide binding tags (LBTs) have been engineered onto the cell surface of *E. coli* to enhance biosorption and recovery of rare earth elements (REEs). The protonation behavior of the bacterial surfaces before and after LBT-display was compared by modeling acid-base titration data. A multiple discrete site, constant capacitance surface complexation model was constructed to examine rare earth (Tb) binding to cell surface functional groups, comparing wild type and LBT-engineered surfaces. Our acid-base titrations show similar pK_a values between the two strains, suggesting induction of LBTs does not significantly alter cell surface protonation behavior. Tb sorption onto the wild type cell surface can be captured by a one-site carboxyl model. The LBT strain exhibited a higher metal loading that can be explained by the increase of sorption sites in the form of lanthanide binding tags. Furthermore, carboxyl site concentrations between wild type and LBT-induced cells were statistically indistinguishable. We thus attribute the engineered strains' increase in Tb adsorption capacity and affinity to the addition of lanthanide binding tags to the cell surface. The Tb stability constant with the LBT site is two orders of magnitude higher than that with the carboxyl functional group. As a result, at low metal loading < 10 μM, the Tb binding to the cell surface of the LBT-strain is controlled by the presence of high-affinity, but lower capacity, LBT sites. At higher metal loadings > 10 μM, a more abundant but low affinity functional group becomes the main source of adsorption that results in an overall higher sorption capacity. This work demonstrates how surface complexation modeling can be implemented for bacterial surfaces engineered with a known protein tag to optimize REE recovery from fluids with variable pH and metal loadings.

Highlights

- Bioengineered *E. coli* display increased sorption capacity and affinity for rare earths.
- Engineered LBT sites have higher affinity for rare earths than wild type surface sites.
- REE-cell surface binding mode depends on both pH and aqueous concentration.

1. Introduction

Rare earth elements (REEs) are essential for clean energy technologies (e.g. wind turbines), consumer products (e.g. smartphone batteries), and military applications (e.g. defense missiles) (Du and Graedel, 2011; Alonso, et al. 2012; Tukker, 2014). In producing REEs, conventional extraction and mining methods can be energetically and chemically intensive, harming the environment through waste production and high energy usage. Liquid-liquid extraction, for example, separates rare earths from other metals based on the reagents' increased selectivity for the lanthanides relative to the other metals. This process, however, can be chemically intensive due to the large amount of organic solvents used in each partitioning step. Rare earth ore deposits consist of mixtures containing variable proportions of REEs (Alonso et al., 2012), including the lanthanides, scandium, and yttrium; in general, however, the heavy lanthanides (HREEs) are of greatest economic importance (Dent, 2012). The extraction and separation of these specific REEs is costly. In response to these technological challenges and associated environmental impacts, we have recently engineered bacteria with high selectivity for REEs, particularly the HREEs, found in geothermal brines and mining and electronic waste leachates (Park et al. 2016, 2017; Jin et al., 2017; Brewer et al., 2019).

The geochemical behavior of the REEs is characterized by their complex speciation behavior, complicating their separation from natural fluids. While all REEs are found predominantly in the +3 oxidation state under Earth surface conditions, they form strong aqueous complexes with numerous anionic species including fluoride, chloride and hydroxide, as well as

carbonate, sulfate, bicarbonate, nitrate, and orthophosphate (Haas, Shock, and Sassani, 1995). Speciation depends strongly on the pH and chemical composition of the source hydrothermal fluids, and in general REE complexation is controlled by Cl^- at acid pH and REE precipitation is controlled by OH^- at neutral to basic pH. The aqueous complexation of REEs tends to increase with increasing temperature, which mobilizes these elements in hydrothermal fluids. Importantly, the REEs can form strong complexes with organic acidic functional groups, particularly carboxylate sites (Kolat 1970). This property leads to the relatively high affinity of REEs for natural microbial cell surfaces (Moriwaki and Yamamoto, 2013), but genetic engineering of the cell surface has been demonstrated to effectively enhance REE adsorption, particularly for the separation of valuable HREEs, in complex solutions (Park et al., 2017).

Scientists have begun expressing lanthanide binding tags (LBTs), short peptides with high affinity for REEs, on bacterial cell surfaces to selectively bind trace rare earth metals (Park et al. 2016,2017). LBT affinity for REEs has been tested under rapid luminescence detection (Nitz et al., 2004) and NMR spectroscopy (Martin et al., 2007). Nitz et al. (2004) show that the Terbium (Tb^{3+}) - LBT complex is in a state of eight coordination by monodentate oxygen ligands of aspartic acid (Asp)1, asparagine (Asn)3, and Asp5, bidentate carboxyl ligands from glutamic acid (Glu)9 and (Glu)12, and the backbone carbonyl group of tryptophan (Trp)7. An analysis of the electrostatic potential further shows a neutrally charged Tb^{3+}-LBT complex despite the positively charged terbium ion and the multitude of negatively charged ligands. The high affinity of the LBT towards rare earths stems from its chemical binding environment, where the peptide-based ligands exclude water from the first coordination sphere. Martin et al. (2007) report another reason for high rare earth affinity of the lanthanide binding tag: The tag is able to mediate alignment between the lanthanide ion and the protein to dramatically lower the mobility

of the complex. Both Nitz and Martin argue for enhanced binding of trivalent rare earths through a unique steric effect between the protein ligands and the metal.

To determine mechanisms of enhanced REE biosorption on engineered cell surfaces, REE complexation by wild type (e.g., non-engineered) cell surfaces must first be understood. Bacteria cell walls are complex and contain multiple types of functional groups, including carboxyl, hydroxyl, phosphoryl (Fein et al., 1997), sulfhydryl (Yu and Fein 2015; Mishra et al. 2017), and amine groups (Borrok, Turner, and Fein, 2005; Guiné et al., 2006). Rare earth element biosorption onto bacterial surfaces has been shown to be predominantly controlled by carboxyl and phosphoryl functional groups (Texier et al. 2000; Markai et al. 2003; Ngwenya et al. 2009; 2010). Findings from time-resolved fluorescence spectroscopy (Texier et al., 2000; Markai et al., 2003; Ozaki et al., 2006) suggest that lanthanide biosorption onto the wild type cell surface occurs through inner-sphere carboxylate binding. Furthermore, Ngwenya et al. (2009) show through EXAFS that phosphoryl groups dominate sorption at lower pH while carboxyl groups dominate sorption at higher pH. Texier et al. (2000) and Takahashi et al. (2005) both suggest that rare earths form inner-sphere complexes with both carboxylate and phosphoryl groups. More specifically, Ngwenya et al. (2010) show that the phosphoryl groups dominate sorption of light and middle rare earths while carboxylate coordination may be favored for some middle and heavy lanthanides. Thus, surface complexation mechanisms vary even within the rare earth series. Moreover, because prior experiments were performed over a limited range of concentrations and surface loadings, the relationship between loading and complexation has not been well studied.

Surface complexation modeling (SCM) has previously been used to characterize REE sorption onto cell surfaces (Markai et al., 2003; Ngwenya et al., 2010). Markai et al. (2003) and

Ngwenya et al. (2010) both use SCM to fit carboxyl-REE or phosphoryl-REE stability constants to experimental sorption edge data ranging from pH 3 to 6.5. Prior to sorption edge modeling, potentiometric titrations, which informs the protonation state of each site type at a given pH, were modeled to obtain pK_a values for carboxyl, phosphoryl, and hydroxyl functional groups. These values typically range from 2-6, 5.65-7.20, and 9.6-10.8 for carboxyl, phosphoryl, and hydroxyl functional groups, respectively (Hong and Brown, 2006). Both studies implement a one-site carboxyl or phosphoryl constant capacitance model in an attempt to best-fit results to experimental sorption edge data. A variety of SCMs have been shown to successfully capture REE sorption as a function of pH, and both a one-site carboxyl model and a one-site phosphoryl model can adequately fit the sorption edge data.

The current study presents sorption isotherm results and implements a surface complexation model for Tb^{3+} adsorption onto engineered bacterial surfaces. Our objective is to develop an SCM that accurately models Tb biosorption onto *E. coli* bacteria both with or without LBTs, allowing us to compare the affinities of wild type and LBT surface site types for Tb. This study presents results from sorption isotherm experiments at a constant pH of 6, the pH of maximum REE adsorption (Park et al., 2016), allowing us to deduce stability constants at the studied pH that apply for a wide range of different metal concentrations in solution. In this manner, we illustrate how addition of different site types due to LBT engineering can alter sorption capacity and the cell surface affinity for Tb under varying metal loadings and pH. This becomes relevant as feedstock from geothermal fluids and mining leachates have highly variable rare earth concentrations. Finally, we will show the partitioning of Tb binding onto different site types over a range of aqueous Tb concentrations, illustrating how a quasi-mechanistic sorption

model could be applied to an engineered bioreactor setup with a wide range of REE inlet concentrations.

2. Methods

2. 1. Cell preparation and harvesting

For a full description of LBT expression see Park et al. (2017). Briefly, the *E. coli* strains harboring a *lpp-ompA*-dLBTx8 expression plasmid was grown in LB media supplemented with 50 μg/mL ampicillin. Expression of *lpp-ompA*-dLBTx8 was induced at mid-exponential phase using 0.002% arabinose for 3 h at 37 °C. Wild type, un-induced (WT) cells contained the *lpp-ompA*-dLBTx8 expression plasmid but were not treated with arabinose. Cells were harvested by centrifugation at 4,000 x*g* for 10 min, washed once in 10 mM MES (2-(N-morpholino)-ethanesulfonic acid) pH 6, and normalized by wet weight for acid/base titrations. Cell suspension densities ranging from 108 to 125 wet grams/L and 32 to 48 wet grams/L were obtained for wild type *E. coli* and dLBTx8 *E. coli*, respectively. Wild type and dLBTx8 cells were massed as wet cell pellets before baking for 24 hr at a temperature of 65 °C. The dry mass of cells were then measured to obtain wet:dry mass ratios for both strains of *E. coli*.

2. 2. Acid/base titration of wild type (WT) and dLBTx8 induced (LBT) strains of E. coli

Triplicate acid-base titrations were conducted on wild type (WT) and dLBTx8 (LBT) strains of *E. coli* cells harvested at mid-exponential phase. The solution was initially acidified with 0.1 M HCl to a pH of 3.5. The bacterial suspension was purged with N_2 gas for thirty minutes before and throughout the titration. A base titration using 0.1 M NaOH titrant was conducted at room temperature using a Titronic 300 automatic titrator. A monotonic equivalence

point titration method was used to add the same volume (0.05 mL) of titrant at each step. This study focuses on a pH range of 3.5–10.0. pH below 3.5 has been shown to irreversibly damage bacteria by displacing structurally bound Mg and Ca (Borrok, Fein, and Kulpa, 2004; Borrok, Turner, and Fein, 2005). Although bacterial surfaces have been cited to have substantial buffering capacity below our studied pH range (Fein et al. 2005), our current titrations avoid lower pH values in order to determine proton and cation exchange properties of surface functional groups on undamaged bacterial cell surfaces. A post-titration bacterial suspension was centrifuged and its supernatant (no biomass) was used to blank-correct all of the net proton charge data (Figure 1, 2) in order to obtain proton charge values of only the bacterial cell surface. Raw titration data were converted to net proton charge values using the expression (Sposito 2016):

(1) $$d\,\sigma_{H,titrant} = \frac{(n_A - [H^+]V) - (n_B - [OH^-]V)}{m_s}$$

Where n_A and n_B are moles of acid and base added, respectively, $[H^+]$ and $[OH^-]$ are measured concentrations of hydronium and hydroxyl ions, V is the total volume of solution, and m_s is the dry weight of the biomass. In converting from wet to dry biomass, a measured wet:dry cell weight ratio of 8:1 was used for the wild type *E. coli*, which is consistent with the estimate in Borrok et al. (2005). For the dLBTx8 cell titration curves, a measured wet:dry cell weight ratio of 14:1 was used.

2. 3. Surface complexation modeling

Site concentrations and protonation equilibrium constants were fit using a PHREEQC-compatible optimization program, PhreePlot. The wild type strain *E. coli* was modeled using 1, 2, 3, and 4-site protonation models based on the following proton dissociation reactions:

(2) $R\text{-}COOH \leftrightarrow R\text{-}COO^- + H^+$

(3) $R\text{-}POH \leftrightarrow R\text{-}PO^- + H^+$

(4) $R\text{-}OH \leftrightarrow R\text{-}O^- + H^+$

(5) $R\text{-}NH_3^+ \leftrightarrow R\text{-}NH_2 + H^+$

where R- is the bacterium the respective functional groups are attached to. Reactions (2), (3), (4), and (5) represent carboxyl, phosphoryl, hydroxyl, and amine deprotonation, respectively. The least number of sites required to constrain the observed protonation behavior was used for the remainder of the modeling.

The many proton-dissociable ligands on the lanthanide binding tag can be attributed to the carboxyl groups present on the side chains of the LBT protein, such as on amino acids Asp1, Asp5, Glu9, and Glu12. Because we do not know the total amount of protonatable carboxyl groups, we allowed for this site density to be optimized based on the following reaction:

(6) $LBT\text{-}COOH \leftrightarrow LBT\text{-}COO^- + H^+$

where LBT- is the lanthanide binding tag peptide and -COOH indicates the side chain carboxyl groups present on the amino acids of the tag.

To account for the Tb-complexing and proton-sorbing ligands on the LBT peptide, we developed a simplified three-proton adsorption/desorption reaction:

(7) $LBT\text{-}OH_3 \leftrightarrow LBT\text{-}O^{-3} + 3\ H^+$

Because Nitz et al. (2004) show that a Tb^{3+}-LBT complex is charge neutral, despite simplifying multiple proton dissociation reactions into a simple three-proton sorption/desorption reaction (7), our expression allows us to adequately describe LBT charge neutrality by either sorption to one Tb^{3+} ion or three H^+ ions.

Associated mass action equations used to optimize fit to titration data are as follows:

(8) $K_1 = \frac{[R-COO^-]a_H{}^+}{[R-COOH]}$

(9) $K_2 = \frac{[R-PO^-]a_H{}^+}{[R-POH]}$

(10) $K_3 = \frac{[R-O^-]a_H{}^+}{[R-OH]}$

(11) $K_4 = \frac{[R-NH_2]a_H{}^+}{[R-NH_3^+]}$

(12) $K_5 = \frac{[LBT-COO^-]a_H{}^+}{[LBT-COOH\ ]}$

(13) $K_6 = \frac{[LBT-O^{-2}]a_H{}^{+2}}{[LBT-OH_2]}$

where K is the conditional stability constant for each given reaction and $a_H{}^+$ is the proton activity. A surface area of 140 m^2/dry grams (Fein et al., 1997), which assumes rod-shaped cells 5.0 μm long and 1.0 μm wide with 10^{10} cells/mL in a 2.5 g/L cell suspension, was used to convert model output site densities in sites/nm^2 to moles/dry gram for each individual titration curve and for subsequent surface complexation modeling.

2. 4. Wild type E. coli (WT) surface complexation model

Our surface complexation models were implemented under a temperature of 24 °C, pH 6, and 10 mM NaCl ionic strength. We initially created a model for Tb sorption onto the wild type, un-induced *E. coli* bacterial surface. The carboxylate group is the most readily deprotonated site type amongst carboxylate, phosphoryl hydroxyl, and amine functional groups at a pH of 6. Furthermore, only a 3-site carboxyl, phosphoryl, and hydroxyl model was required for optimal titration modeling. This is likely because, as Hong and Brown (2006) suggest, gram-negative bacteria such as *E. coli* are more likely to possess hydroxyl groups compared to amine groups. We thus investigated Tb sorption using a three-site carboxyl, phosphoryl, and hydroxyl

protonation model, with Tb sorption being accounted for only via carboxyl functional groups (herein after called a 1-site wild type carboxyl model). TRLFS and EXAFS studies (Texier et al., 2000; Takahashi et al., 2005) only find carboxyl- and phosphoryl-REE binding modes, so we assume that hydroxyl groups do not significantly contribute to Tb complexation at the relevant range of pH (pH 3.5 to 6; Brewer et al., 2019). Furthermore, below pH ~6.9, phosphoryl groups are mostly protonated while carboxyl groups are the most prevalent anionic surface site. We thus invoke a 1-site carboxyl binding mechanism for Tb. In addition to Tb complexation to the native carboxyl site, protonation equilibrium constants for all three site types were accounted for based on modeling of the acid-base titration experiment.

The following reaction for wild type *E. coli* Tb sorption was used:

(14) $R\text{-}COO^- + Tb^{3+} \leftrightarrow R\text{-}COOTb^{2+}$

Wild type carboxyl sites were assumed to form monodentate surface complexes with Tb^{3+} cations (Texier et al., 2000). However, we note that it has been suggested that multidentate binding could be possible (Ozaki et al., 2006). The Tb-carboxyl stability constant was optimized and solved for by fitting to Tb adsorption capacity experimental data. More specifically, Tb adsorption capacity data were converted to surface excess (*n*) and equilibrium Tb concentration (*c*) values to compute distribution coefficient (K_d) values through the following expressions:

(15) $$n = \frac{\mu mol\ of\ Tb\ sorbed}{dry\ grams\ of\ biomass}$$

(16) $$c = Tb\ added\ (\mu M) - Tb\ sorbed\ (\mu M)$$

(17) $$K_d = \frac{n}{c}$$

We optimized Tb stability constants based on experimental *n* and K_d values to yield the best overall fit to both experimental sorption capacity and sorption affinity. While fitting to *n* can be useful to match experimental sorption capacity results, fitting to K_d can yield more accurate

results at low surface loadings. Thus, when optimizing for Tb stability constants, we pooled *n* and K_d experimental values and optimized to both values. Uncertainties on fitted stability constants are estimated using bounds computed by optimizing carboxyl-Tb stability constants to experimental surface excess and distribution coefficient data $\pm$ 1 standard deviation. In propagating error associated with a fixed site concentration obtained from titration fitting, $\pm$ 1 standard deviation of the calculated carboxyl site concentration from the acid-base titration modeling was also applied while fitting to surface excess and distribution coefficient data. In this way, we establish the maximum range of values that can be obtained via optimization of the carboxyl-Tb stability constant accounting for $\pm$1 standard deviation of experimental surface excess, distribution coefficient, and titration modeling error.

2. 5. LBT E. coli surface complexation model

In addition to a wild type 1-site carboxyl model, we created an LBT + native carboxyl site model wherein LBT-O^{-3}, LBT-carboxyl, native carboxyl, phosphoryl, and hydroxyl sites can exchange protons, but only $LBTO^{-3}$ sites and native carboxyl groups participate in metal complexation. Native carboxyl-Tb biosorption was accounted for using reaction (14) and LBT-Tb biosorption was accounted for using a simplified 1:1 monodentate reaction:

(18) LBT-O^{3-} + Tb^{3+} $\leftrightarrow$ LBT-OTb^{0}.

Although Tb^{3+}-LBT complexes are eight-point coordinated (Nitz et al. 2004), we consolidated the polydentate Tb binding into a single Tb binding constant following Nitz et al. (2004). All remaining proton dissociable sites on the LBT (expressed by reaction 6) were initially allowed to complex Tb. However, we find that Tb complexation to these LBT-COO^{-} sites causes a dramatic overestimation in modeled adsorption of Tb under all conditions.

Preventing these LBT-COO^- sites from participating in Tb complexation yields an adequate match to experimental surface excess and distribution coefficient data (Section 3.2). We hypothesize that proton dissociable LBT-COO^- sites do not participate in Tb complexation due to an allosteric inhibition mechanism in which the carboxyl groups present on LBT protein sub-units are in a conformation that is inactive to metal-binding. Chakravorty et al. (2013) use molecular dynamics methods and nuclear magnetic resonance structure determination to illustrate how zinc coordination is allosterically inhibited in the protein CzrA of *Staphyloccocus aureus*. Furthermore, Cook et al. (2019) invoke a similar allosterically inhibited yttrium binding mechanism for carboxylate ligands present on the high-affinity lanthanide-binding protein, Lanmodulin, present in *Methylobacterium extorquens*.

Similar to the WT model, the model describing dLBTx8 induced *E. coli* cells uses a surface area of 140 m^2/gram dry cell weight. The concentration of $LBTOH_3$ sites was fixed at 5.93×10^{-5} $\frac{\text{moles}}{\text{dry gram}}$ based on estimates of the number of dLBTx8 peptides induced onto the outer membrane protein A (Supplemental Information 1). The LBT-Tb stability constant was optimized to best fit experimentally determined values of both *n* and K_d. We then compared the obtained value with a value of 7.24 reported in Nitz et al. (2004) and with our optimized value for wild type *E. coli* – Tb binding.

2. 6. Treatment of electrostatic potential of bacterial surfaces

The presence of charged complexes and adsorbed ions on surfaces generates surface charge, which impacts the thermodynamic affinity of surface complexation reactions (Goldberg 1992). Previous studies have implemented a constant capacitance model (CCM) approach, allowing the capacitance parameter (C) to be optimized in order to create a better model fit with

experimental sorption data (Fein et al., 1997). This approach is limited because it relates surface charge to surface potential using a C value that is unconstrained in optimization and relies on only the curve-fitting procedure without external physiological validation. Some studies approach electrostatics as playing a much smaller role in bacterial sorption behavior compared to other parameters such as site density, surface area, and functional group pK_as (Borrok, Turner, and Fein, 2005). Despite the limitation of a constant capacitance model, we adopt a CCM approach in this study to importantly account for the high valence of lanthanides when sorbed to the wild type bacterial surface sites. Not accounting for electrostatics using any charge model (e.g., a non-electrostatic model) would pose an even more troubling assumption that charge build-up from lanthanide biosorption is negligible. In this study the capacitance value in the CCM was fixed to 8.0 $\frac{F}{m^2}$ based on optimization calculations conducted by Fein et al. (1997). Furthermore, Ngwenya et al (2009, 2010) use this 8.0 $\frac{F}{m^2}$ capacitance value in calculating REE-bacteria stability constants. By using the same capacitance parameter, we maintain consistency with past sorption studies, allowing us to compare our calculated Tb-carboxyl binding constant with values calculated by others.

3. Results and Discussion

3. 1. Acid-base properties of wild type and engineered cell surfaces.

Wild type *E. coli* acid-base titration data were fit using models containing a range of one to four site types (Figure 1). One and two site types did not adequately capture the protonation behavior of the cells, while three and four site types fit to experimental data equally well. To minimize the number of unconstrained pK_a and site concentration values, a three-site model was used for the wild type strain in a similar fashion as Ngwenya et al. (2009, 2010), accounting for

the protonation reactions given in Eqs. (2)-(4). The exclusion of the amine group in favor of 3 site types (carboxyl, phosphoryl, and hydroxyl) is consistent with Hong and Brown (2006), who demonstrate through isoelectric point and potentiometric titration measurements that the high pK_a site is more likely a hydroxyl and not an amine group for gram-negative bacteria such as *E. coli*. The fourth and fifth reactions given in Eq. (6) and (7) are incorporated to model the protonation behavior of the dLBTx8 induced *E. coli* strain. Fitted site concentrations and pK_a values obtained from modeling fits to titration data for the 3-protonation site carboxyl WT model and the 5-protonation site LBT + native carboxyl model are given in Table 1 and Figure 2. Standard deviations are calculated based on modeling results obtained from titration experiments for a given strain run in triplicate. The total site concentrations we computed fall within an appropriate range of total moles of sites/dry gram compared to values found in the literature (Table 1). The total sites on the WT cells are notably similar to the multisite Langmuir model developed by Martinez et al. (2014) that uses a linear programming regression method (LPM) to solve for site densities based on REE sorption data.

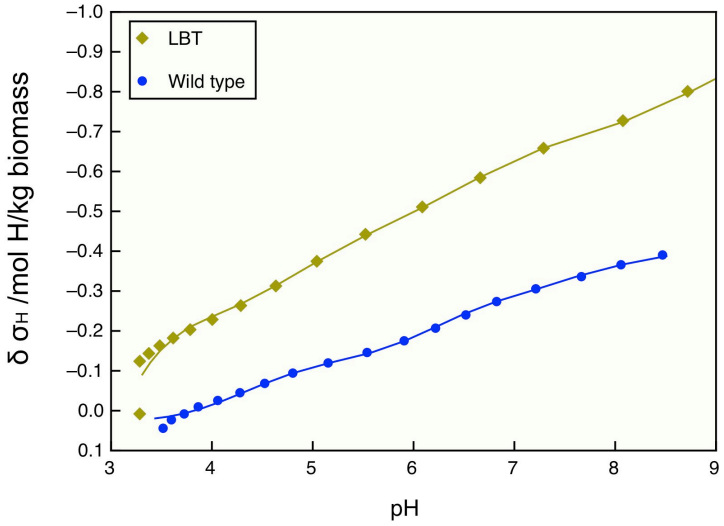

Figure 1. Wild type *E. coli* CCM acid/base titration data (black symbols) and model fits for a typical titration experiment. Models with varying amounts of proton-dissociable site types are shown as curves.

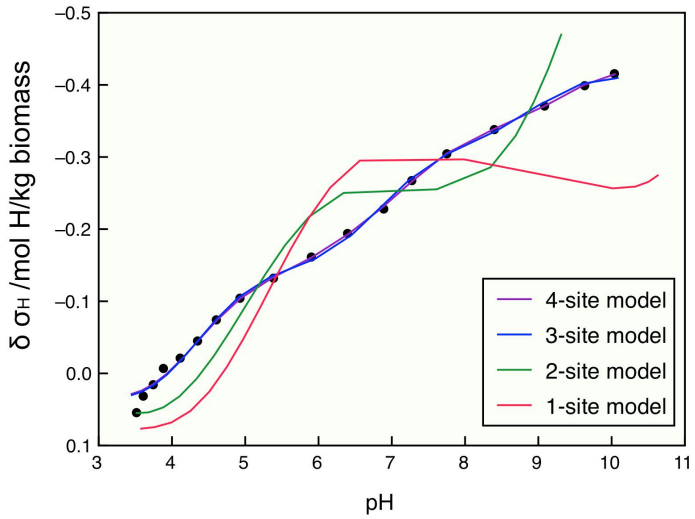

Figure 2. Averaged experimental data of acid/base titrations run in triplicate (filled symbols) with corresponding 3-protonation site wild type and 4-protonation site LBT *E. coli* CCMs (curves). Site concentrations and pK_a's for the modeling fits to titrations are given in Table 1. The 3-protonation site wild type CCM contains carboxyl, phosphoryl, and hydroxyl site types while the 5-protonation site LBT CCM contains the same site types but also includes a lanthanide binding tag – carboxyl site type and an $LBTO^{-3}$ site type.

Table 1. Total site concentrations and pK_as of various models describing bacterial surface protonation of wild type and LBT-displayed *E. coli*. Sites 1, 2, 3 and 4 are attributed to the proton-dissociable carboxyl, phosphoryl, hydroxyl and LBT binding sites corresponding to protonation reactions given in Eqs. (2), (3), (4), and (6), respectively.

Model Type	Site concentrations (mol sites/dry gram × 10^{-4})					pK_a			
	Site 1	Site 2	Site 3	Site 4[a]	Total	Site 1	Site 2	Site 3	Site 4
multisite Langmuir Martinez et al. (2014)	n/a	n/a	n/a	n/a	5.49	n/a	n/a	n/a	n/a
4-protonation site non-electrostatic Borrok et al. (2005)	8.80±0.56	7.28±3.04	4.24±1.68	5.28±2.4	25.6	3.1	4.7	6.6	9.0
5-protonation site CCM (LBT) [this work]	1.97±0.56	1.78±0.49	1.96 ±0.79	0.80±0.59*	7.10±1.23	4.98±0.13	6.82±0.29	9.15±0.70	4.86±0.20
3-protonation site CCM (wild type) [this work]	1.53±0.07	1.37±0.52	0.75±0.14	n/a	3.65 ± 0.54	4.23±0.05	6.68±0.10	9.01±0.28	--
3-protonation site CCM Ngwenya et al. (2003)	5.0±0.7	2.2±0.6	5.5±2.2	n/a	12.7	4.3±0.2	6.9±0.5	8.9±0.5	--
3-protonation site CCM Fein et al. (1997)	1.20	4.40	5.20	n/a	10.8	4.82±0.14	6.9±0.5	9.4±0.6	--

[a]Site 4 for a 4-site non-electrostatic model (Borrok et al, 2005) refers to a naturally-occurring fourth site type, while for our 5-site CCM (LBT), it refers to the engineered LBT site's carboxyl moieties present on amino acid side chains. The 5-site CCM (LBT)'s 5th site type is a $LBTO^{-3}$ site type (reaction 7) with a fixed site density of 0.59 mol/dry g and an optimized pK_a of 9.96±0.10.

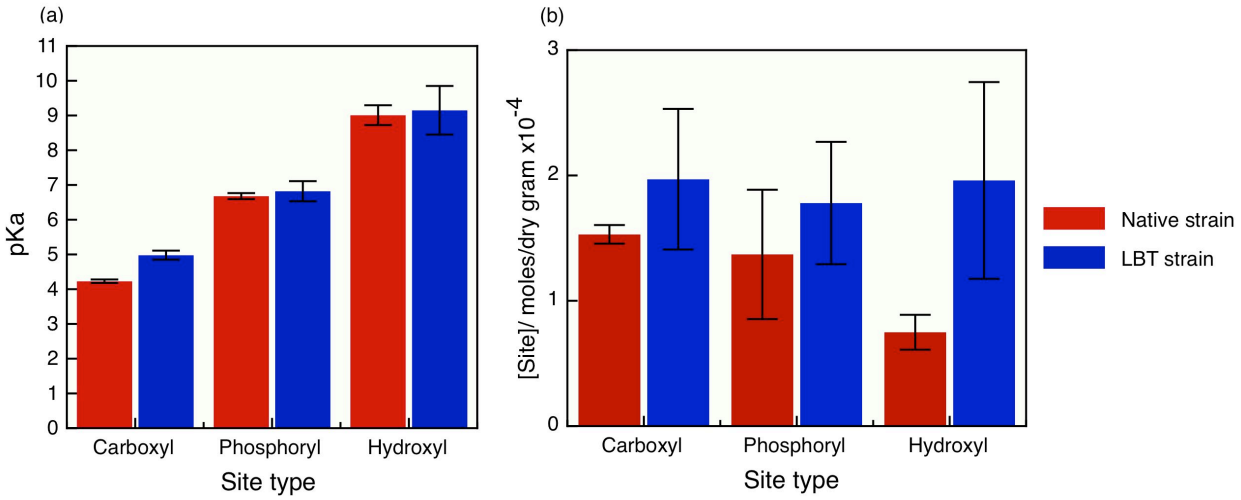

Figure 3. Fitted pK_a and site concentration values for wild type and LBT strains of *E. coli* based on surface complexation modeling of acid/base titration data. Error bars indicate ±1 standard deviation as calculated by triplicate experiments.

Phosphoryl (Site 2) and hydroxyl (Site 3) pK_a values are within error between the two strains, while carboxyl group pK_as between strains are both reasonable values for the carboxyl moiety (Hong and Brown 2006). This suggests that the induction of LBTs does not significantly alter the inflection points in the acid-base titration of the *E. coli* surface. A two-sample t-test assuming unequal variances was performed for carboxyl, phosphoryl and hydroxyl site concentrations, with a null hypothesis that for each site type, the mean site concentration difference between WT and LBT strains was 0. Using $p < 0.05$, the resultant t stat values for carboxyl, phosphoryl, and hydroxyl site types were -1.33, -1.00, and 2.63, respectively. As the two-tailed t critical values for carboxyl, phosphoryl, and hydroxyl site types were 4.30, 2.78, and 4.30, respectively, we cannot reject the null hypothesis for any of the sites. Mean carboxyl, phosphoryl, and hydroxyl site concentrations are statistically indistinguishable between WT and LBT strains. Figure 3 illustrates the differences in fitted pK_a and site concentration values between the wild type and engineered bacterial strains, with error bars indicating $\pm$ 1 standard deviation.

3. 2. Surface complexation modeling of Tb adsorption isotherms

3. 2. 1. One-site native carboxyl model describing Tb sorption onto wild type *E. coli* cells

Markai et al. (2003) and Ngwenya et al. (2010) use a one-site CCM to study lanthanide sorption onto the gram-positive bacteria, *Bacillus subtilis,* and the gram-negative bacteria, *Pantoea agglomerans*, respectively, as it has been postulated that the carboxyl functional group dominates sorption in the pH range of 5-6 (Takahashi et al., 2010). Although it is clear from our titration data that multiple types of proton-dissociable surface functional groups are present on the wild type cell surfaces, it is not clear whether all site types contribute substantively to REE

adsorption. To determine whether a single metal exchangeable site is sufficient to capture REE adsorption data, we applied a 1-REE site carboxyl CCM (WT model in Figure 4) with a fixed pK_a of 4.23 and site concentration of $1.53 \pm 0.07 \times 10^{-4}$ $\frac{\text{moles}}{\text{dry gram}}$ to fit our Tb adsorption isotherm data. This 1-REE site carboxyl CCM incorporates the Tb-carboxyl surface complexation reaction given in Eq. (14) in addition to the protonation reactions given in Eqs. (2)-(4). Optimization of the wild type 1-REE site carboxyl model to fit experimental distribution coefficient, K_d, and surface excess, *n*, values resulted in a carboxyl-Tb stability constant of 5.12 [5.00, 5.25] (with a lower bound of 5.00 and an upper bound of 5.25). Optimization to a pooled dataset of *n* and K_d values results in a good holistic fit to sorption capacity (*n* vs *c*) and sorption affinity (K_d vs *n*) plots (Figure 4a,b). A one-REE site carboxyl model was sufficient in capturing the total Tb sorption capacity of the wild type *E. coli* surface.

Table 2. 1-REE site carboxyl wild type and 2-REE site LBT plus carboxyl CCM parameters used in addition to the protonation parameters in Table 1 to model Tb binding data.

Model Type	Site Type	Site-Tb $\log_{10}K$	Site concentration (moles/dry gram x 10^{-4})
Wild type model			
	Carboxyl	5.12* [5.00, 5.25]	1.53±0.07
LBT model			
	Carboxyl	5.12*	1.97±0.56
	LBT	7.51 [7.01, 8.56]	0.59

*Carboxyl-Tb stability constant fixed from the carboxyl-Tb $\log_{10}K$ constant obtained from the wild type model

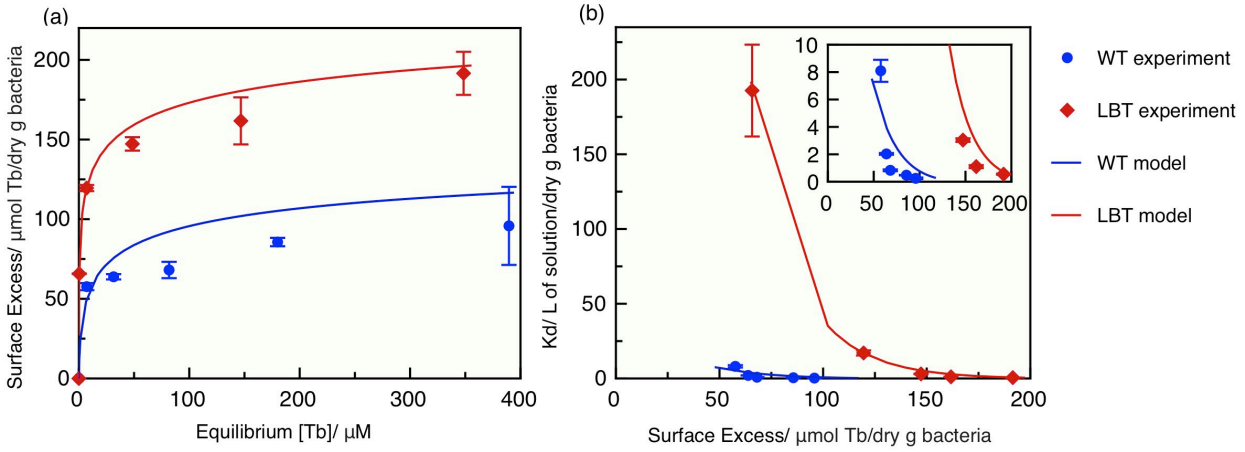

Figure 4. Sorption isotherm and distribution coefficient modeling fit at a pH of 6. Wild type (WT) model refers to a 1-site carboxyl model describing the sorption of Tb to the wild type strain. The WT model shown here was fit to a pooled surface excess and distribution coefficient dataset. The LBT model refers to a native carboxyl and lanthanide binding tag model describing the sorption of Tb to the LBT strain. Experimental data have been previously published in Park et al. (2017).

Our Tb-carboxyl stability constant estimate of 5.12 [5.00, 5.25] is two orders of magnitude higher than *Enterobacteriaceae* Zn-carboxyl binding ($\log_{10}K$ = 3.3±0.1) and one order of magnitude higher than Pb-carboxyl binding ($\log_{10}K$ = 3.9±0.8) (Ngwenya, Sutherland, and Kennedy 2003). This suggests that the wild type carboxyl group may be more selective for Tb compared to some heavy metals. In order to recover REEs from environmental fluids containing a mixture of competing metals such as Pb, we require a higher-affinity site type to increase the selectivity of the surface for REEs. Our calculated average $\log_{10}K$ of 5.12 for Tb binding is comparable to reported stability constants of 5.37 and 4.95 reported in Ngwenya et al. (2010) and Martinez et al. (2014) respectively. Thus, we conclude that a one-site carboxyl CCM is sufficient to model Tb sorption onto the wild type *E. coli* cell surface at pH 6 and for Tb aqueous concentrations up to 1.30 mmol/dry g bacteria in this study.

3. 2. 2. LBT and native carboxyl site model describing Tb sorption onto dLBTx8 induced *E. coli* cells

To model adsorption data for the dLBTx8 induced strain of *E. coli*, we implement a bottom-up approach and superimpose Tb binding by LBTs while assuming the interaction between a native carboxyl group and a Tb ion to be the same for the wild type and engineered strains. Surface protonation reactions given in Eqs. (2)-(4), (6), and (7) and Tb-complexation reactions given in Eqs. (14) and (18) are all included in the SCM. We fix the carboxyl-Tb stability constant at our previously calculated value of 5.12 [5.00, 5.25] from the wild type 1-REE site model and optimize for the LBT-Tb binding constant. We obtain a value of 7.51 [7.01, 8.56] – we attribute the large upper and lower bound range to the propagation of error carried over from carboxyl-Tb stability constant and carboxyl site concentration uncertainties. Our average LBT-Tb binding constant of 7.51 is remarkably similar to 7.24 reported by Nitz et al. (2004). Moreover, the average LBT-Tb stability constant of 7.51 is two orders of magnitude higher than the average carboxyl-Tb binding constant of 5.12, highlighting the substantially higher affinity of LBT sites for REEs compared to wild type carboxyl sites. We initially incorporated LBT-COO binding to Tb, but the resultant model isotherm (not shown) dramatically overestimated adsorption, yielding a maximum surface excess of ~260 μmol/dry g bacteria. Because the maximum sorption determined by experiments is closer to ~200 μmol/dry g bacteria, we removed the LBT-COO-Tb binding reaction. The resultant model can be found in Figure 4 – allowing only native carboxyl and $LBTO^{-3}$ groups to bind Tb yields an excellent fit to both experimental surface excess and distribution coefficient data. Similar to Cook et al. (2019), we explain the LBT-COO sites' inability to bind Tb to allosteric inhibition, wherein the carboxyl ligands are in a conformation that is inactive to the binding of certain metals.

A major advantage of implementing a quasi-mechanistic modeling approach compared to pure empirical adsorption modeling is our ability to distinguish chemical features of the surface and conditions of the aqueous solution that favor REE recovery. Our SCM results can be used to infer dominant surface Tb speciation as a function of aqueous concentration (Figure 5). Overall, LBT sites dominate Tb surface complexes at low aqueous concentrations, while native cell surface functional groups become dominant at higher loadings, once LBT sites become saturated. At aqueous Tb concentrations exceeding 20 µmol/dry gram bacteria, carboxyl sites play an equal or greater role in sorption of Tb than the more Tb selective LBTs. Thus, both pH and equilibrium Tb concentration influence surface speciation. Such insights will be useful in interpreting the results of spectroscopic techniques such as EXAFS and TRLFS, which have yielded varying conclusions as to whether carboxyl or/and phosphoryl functional groups act as the dominant sorption site of REEs. Texier et al. (2000) conducted TRLFS on *P. aueruginosa* exposed to high concentrations of Eu (8 mM) at pH 5 and concluded that binding occurs on both carboxyl and phosphoryl groups. At lower Eu concentrations (up to 500 µM) at the same pH, Markai et al. (2003) report that binding by carboxylate alone is sufficient to describe Eu sorption on *B. subtilis*. Thus, we hypothesize that at pH ~5-6, carboxyl groups are the dominant sorption site at low to intermediate aqueous REE concentrations, while at higher concentrations (>~1mM), both carboxyl and phosphoryl groups contribute significantly to REE complexation.

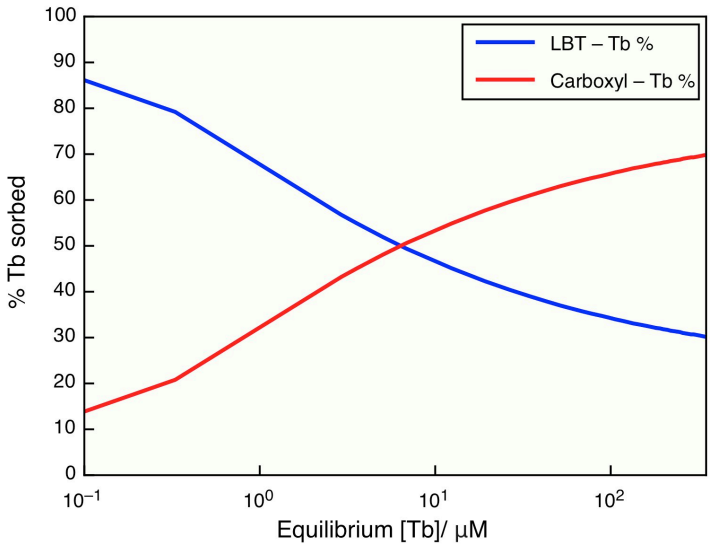

Figure 5. Percent Tb sorbed to LBT and carboxyl sites calculated from LBT model at a pH of 6 as a function of equilibrium Tb concentration, using a cell suspension density of 0.36 dry g bacteria/L. At low loadings of < 10^1 μM, lanthanide binding tag sites dominate Tb sorption, while at higher loadings > 10^1 μM, carboxyl groups play a large role in Tb sorption due to the saturation of LBT sites.

3. 2. 3. Optimal Tb recovery as a function of pH and equilibrium aqueous concentration

From an REE recovery and product purity standpoint, it is advantageous to design conditions of the bioreactor or flow system that maximize the fraction of REEs sorbed (and specific REE type) to LBTs compared to other surface site types, while minimizing sorption of non-REE metals. Conditions that optimize for separation may compromise overall recovery, so striking the right balance requires a quantitative exploration of parameter space that is not realistic to access using experiments alone. Figure 6 gives a plot of % Tb recovered as a function of equilibrium aqueous concentration and pH. Based on our results in simple buffered solutions at a 10 mM ionic strength and 24 °C temperature, low equilibrium Tb concentrations likely provide for optimal REE recovery at the studied pH range of 3 to 8. Due to the high pK_a of 9.96 of lanthanide binding tag sites, changes in pH from 3 to 8 have a minimal effect on LBT-Tb sorption behavior under low equilibrium Tb concentrations. However, at higher loadings of ~690 μmol/dry g bacteria, when LBT sites are saturated and carboxyl groups are the dominant sorbing site type, a pH of 6 provides optimal % Tb recovery. Thus, we demonstrate how both pH and equilibrium Tb aqueous concentrations are important factors in understanding what parameter space achieves most efficient recovery of rare earths. Our future work focuses on extending this SCM to account for other species that compete with the REEs for surface sites, as well as to predict selectivity among the REEs, both in batch adsorption mode and under flow. As temperature can dramatically affect the thermodynamics of aqueous and surface reactions, future

work should also investigate sorption behavior of engineered cells at elevated temperatures consistent with environmental samples from geothermal brines. Sorption isotherms with changing temperature would allow for the development of temperature-dependent stability constants for REE binding.

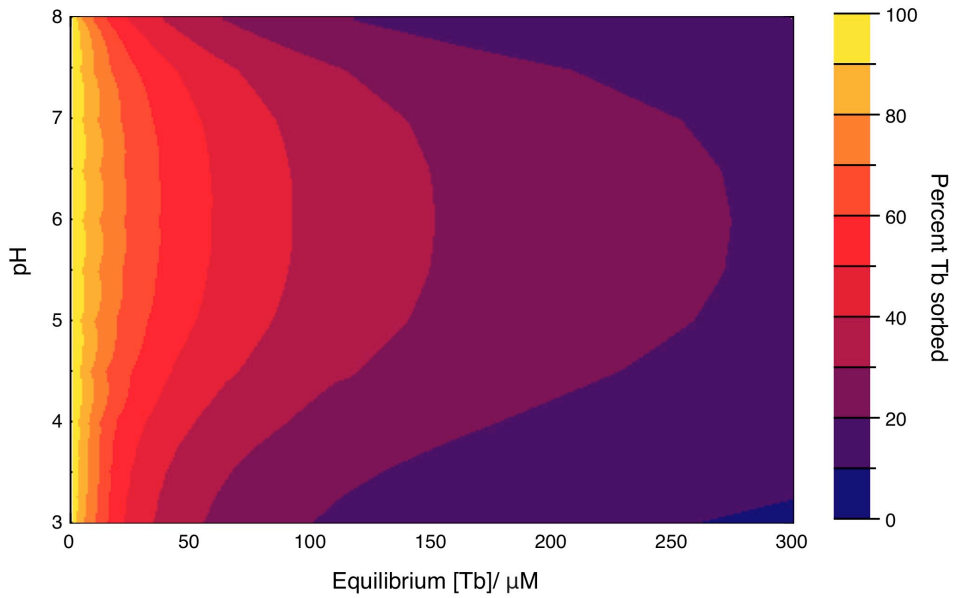

Figure 6. Percent Tb sorbed to LBT-engineered bacterial surface (adsorption to both carboxyl and lanthanide binding tag sites) calculated from LBT model as a function of pH and aqueous Tb concentration, using a cell suspension density of 0.36 dry g bacteria/L. Optimal sorption for low metal loadings occurs at all pH (3-8), while optimal sorption for higher metal loadings (~250 µM) occurs at a pH of ~6.

4. Conclusions

We report that the incorporation of LBTs into the *E. coli* outer membrane poses two major benefits: (1) Sorption onto lanthanide binding tags increases REE selectivity and affinity of the cell surface, which is relevant at low metal loadings, and (2) the presence of these tags increases the total concentration of available sorption sites, thereby also increasing overall adsorption capacity. Tb binding is controlled by the presence of high-affinity, but low capacity, lanthanide binding tags as well as lower-affinity, but more abundant, wild type functional groups that increase overall sorption capacity at higher aqueous REE concentrations.

In this study, we observe the wild type *E. coli* surface complexation of Tb at a pH of 6 to be well modeled with a monodentate carboxylate binding mechanism. We propose a new surface complexation model for studying lanthanide binding tag sorption of Tb to *E. coli* through a constant capacitance model electrostatic treatment and monodentate binding mode simplification of LBTs. We observe that cells with lanthanide binding tags possess both high-affinity LBT sites and lower-affinity wild type functional groups. Protonation behavior and site concentrations of adsorbing, native carboxyl functional groups were indistinguishable between WT and LBT strains. We thus attribute an increase in Tb sorption affinity and capacity to the presence of lanthanide binding tags on the cell surface. Future work will focus on studying the competition for engineered and wild type surface sites in the presence of other naturally occurring metals, such as Cu, Mg, and Pb, found in geothermal brines and mining leachates. Further work should also be conducted on desorption studies in order to optimize removal of rare earths from bacterial surfaces once biosorption has occurred (Bonificio and Clarke 2016).

5. Acknowledgements

This research is supported by the U.S. Department of Energy, Office of Energy Efficiency and Renewable Energy, Geothermal Office. The work was performed in part under the auspices of the U.S. Department of Energy by Lawrence Livermore National Laboratory under Contract DEAC52-07NA27344 (LLNL-JRNL-774812). EC acknowledges support from the National Science Foundation Graduate Research Fellowship under Grant No. 1752814. EC would also like to thank Jennifer Mills for her discussion and continual feedback throughout this project. The authors declare no competing financial interest.

References

Alonso, Elisa, Andrew M. Sherman, Timothy J. Wallington, Mark P. Everson, Frank R. Field, Richard Roth, and Randolph E. Kirchain. 2012. "Evaluating Rare Earth Element Availability: A Case with Revolutionary Demand from Clean Technologies." *Environmental Science and Technology* 46 (6): 3406–14. https://doi.org/10.1021/es203518d.

Bonificio, William D., and David R. Clarke. 2016. "Rare-Earth Separation Using Bacteria." *Environmental Science and Technology Letters* 3 (4): 180–84. https://doi.org/10.1021/acs.estlett.6b00064.

Borrok, David, Jeremy B. Fein, and Charles F. Kulpa. 2004. "Proton and Cd Adsorption onto Natural Bacterial Consortia: Testing Universal Adsorption Behavior." *Geochimica et Cosmochimica Acta* 68 (15): 3231–38. https://doi.org/10.1016/j.gca.2004.02.003.

Borrok, David, Benjamin F. Turner, and Jeremy B. Fein. 2005. "A Universal Surface Complexation Framework for Modeling Proton Binding onto Bacterial Surfaces in Geologic Settings." *American Journal of Science* 305 (6-8 SPEC. ISS.): 826–53. https://doi.org/10.2475/ajs.305.6-8.826.

Brewer, A., Chang, E., Park, D.M., Kou, T., Li, Y., Lammers, L.N. and Jiao, Y. (2019) Recovery of Rare Earth Elements from Geothermal Fluids through Bacterial Cell Surface Adsorption. *Environmental Science & Technology* 53, 7714-7723. https://doi.org/10.1021/acs.est.9b00301

Brewer, A., Dohnalkova, A., Shutthanandan, V., Kovarik, L., Chang, E., Sawvel, A., Mason, H., Reed, D., Ye, C. and Hynes, W. (2019) Microbe Encapsulation for Selective Rare Earth Recovery from Electronic Waste Leachates. *Environmental Science & Technology*.

https://doi.org/10.1021/acs.est.9b04608

Chakravorty, Dhruva K., Bing Wang, Chul Won Lee, Alfredo J. Guerra, David P. Giedroc, and Kenneth M. Merz. 2013. "Solution NMR Refinement of a Metal Ion Bound Protein Using Metal Ion Inclusive Restrained Molecular Dynamics Methods." *Journal of Biomolecular NMR* 56 (2): 125–37. https://doi.org/10.1007/s10858-013-9729-7.

Cook, Erik C., Emily R. Featherston, Scott A. Showalter, and Joseph A. Cotruvo. 2019. "Structural Basis for Rare Earth Element Recognition by Methylobacterium Extorquens Lanmodulin." Research-article. *Biochemistry* 58 (2): 120–25. https://doi.org/10.1021/acs.biochem.8b01019.

Dent, Peter C. 2012. "Rare Earth Elements and Permanent Magnets (Invited)." *Journal of Applied Physics* 111 (7): 1–6. https://doi.org/10.1063/1.3676616.

Du, Xiaoyue, and T. E. Graedel. 2011. "Global In-Use Stocks of the Rare Earth Elements: A First Estimate." *Environmental Science and Technology* 45 (9): 4096–4101. https://doi.org/10.1021/es102836s.

Fein, Jeremy B., Jean François Boily, Nathan Yee, Drew Gorman-Lewis, and Benjamin F. Turner. 2005. "Potentiometric Titrations of Bacillus Subtilis Cells to Low PH and a Comparison of Modeling Approaches." *Geochimica et Cosmochimica Acta* 69 (5): 1123–32. https://doi.org/10.1016/j.gca.2004.07.033.

Fein, Jeremy B., Christopher J. Daughney, Nathan Yee, and Thomas A. Davis. 1997. "A Chemical Equilibrium Model for Metal Adsorption onto Bacterial Surfaces." *Geochimica et Cosmochimica Acta* 61 (16): 3319–28. https://doi.org/10.1016/S0016-7037(97)00166-X.

Goldberg, S. 1992. "ScienceDirect - Advances in Agronomy : Use of Surface Complexation Models in Soil Chemical Systems." *Advances in Agronomy*.

http://linkinghub.elsevier.com/retrieve/pii/S0065211308604927%5Cnpapers2://publication/uuid/01C9419F-EEDD-41C0-B69D-7F9DCA1404F7.

Guiné, V., L. Spadini, G. Sarret, M. Muris, C. Delolme, J. P. Gaudet, and J. M.F. Martins. 2006. "Zinc Sorption to Three Gram-Negative Bacteria: Combined Titration, Modeling, and EXAFS Study." *Environmental Science and Technology* 40 (6): 1806–13. https://doi.org/10.1021/es0509811.

Haas, Johnson R., Everett L. Shock, and David C. Sassani. 1995. "Rare Earth Elements in Hydrothermal Systems: Estimates of Standard Partial Molal Thermodynamic Properties of Aqueous Complexes of the Rare Earth Elements at High Pressures and Temperatures." *Geochimica et Cosmochimica Acta* 59 (21): 4329–50. https://doi.org/10.1016/0016-7037(95)00314-P.

Hong, Yongsuk, and Derick G. Brown. 2006. "Cell Surface Acid-Base Properties of Escherichia Coli and Bacillus Brevis and Variation as a Function of Growth Phase, Nitrogen Source and C:N Ratio." *Colloids and Surfaces B: Biointerfaces* 50 (2): 112–19. https://doi.org/10.1016/j.colsurfb.2006.05.001.

Jin, H., Park, D.M., Gupta, M., Brewer, A.W., Ho, L., Singer, S.L., Bourcier, W.L., Woods, S., Reed, D.W. and Lammers, L.N. (2017) Techno-economic Assessment for Integrating Biosorption into Rare Earth Recovery Process. *ACS Sustainable Chemistry & Engineering* 5, 10148-10155.

Kolat, Robert Stanley. 1970. "A Study of the Rare-Earth Metal Complexes," no. 1961.

Markai, S., Y. Andrès, G. Montavon, and B. Grambow. 2003. "Study of the Interaction between Europium (III) and Bacillus Subtilis: Fixation Sites, Biosorption Modeling and Reversibility." *Journal of Colloid and Interface Science* 262 (2): 351–61.

https://doi.org/10.1016/S0021-9797(03)00096-1.

Martin, Langdon J., Martin J. Hähnke, Mark Nitz, Jens Wöhnert, Nicholas R. Silvaggi, Karen N. Allen, Harald Schwalbe, and Barbara Imperiali. 2007. "Double-Lanthanide-Binding Tags: Design, Photophysical Properties, and NMR Applications." *Journal of the American Chemical Society* 129 (22): 7106–13. https://doi.org/10.1021/ja070480v.

Martinez, Raul E., Olivier Pourret, and Yoshio Takahashi. 2014. "Modeling of Rare Earth Element Sorption to the Gram Positive Bacillus Subtilis Bacteria Surface." *Journal of Colloid and Interface Science* 413: 106–11. https://doi.org/10.1016/j.jcis.2013.09.037.

Mishra, Bhoopesh, Elizabeth Shoenfelt, Qiang Yu, Nathan Yee, Jeremy B. Fein, and Satish C.B. Myneni. 2017. "Stoichiometry of Mercury-Thiol Complexes on Bacterial Cell Envelopes." *Chemical Geology* 464: 137–46. https://doi.org/10.1016/j.chemgeo.2017.02.015.

Moriwaki, Hiroshi, and Hiroki Yamamoto. 2013. "Interactions of Microorganisms with Rare Earth Ions and Their Utilization for Separation and Environmental Technology." *Applied Microbiology and Biotechnology* 97 (1): 1–8. https://doi.org/10.1007/s00253-012-4519-9.

Ngwenya, Bryne T., Marisa Magennis, Valerie Olive, J. Fred W. Mosselmans, and Robert M. Ellam. 2010. "Discrete Site Surface Complexation Constants for Lanthanide Adsorption to Bacteria as Determined by Experiments and Linear Free Energy Relationships." *Environmental Science and Technology* 44 (2): 650–56. https://doi.org/10.1021/es9014234.

Ngwenya, Bryne T., J. Fred W. Mosselmans, Marisa Magennis, Kirk D. Atkinson, Janette Tourney, Valerie Olive, and Robert M. Ellam. 2009. "Macroscopic and Spectroscopic Analysis of Lanthanide Adsorption to Bacterial Cells." *Geochimica et Cosmochimica Acta* 73 (11): 3134–47. https://doi.org/10.1016/j.gca.2009.03.018.

Ngwenya, Bryne T., Ian W. Sutherland, and Lynn Kennedy. 2003. "Comparison of the Acid-

Base Behaviour and Metal Adsorption Characteristics of a Gram-Negative Bacterium with Other Strains." *Applied Geochemistry* 18 (4): 527–38. https://doi.org/10.1016/S0883-2927(02)00118-X.

Nitz, Mark, Manashi Sherawat, Katherine J. Franz, Ezra Peisach, Karen N. Allen, and Barbara Imperiali. 2004. "Structural Origin of the High Affinity of a Chemically Evolved Lanthanide-Binding Peptide." *Angewandte Chemie - International Edition* 43 (28): 3682–85. https://doi.org/10.1002/anie.200460028.

Ozaki, Takuo, Yoshinori Suzuki, Takuya Nankawa, Takahiro Yoshida, Toshihiko Ohnuki, Takaumi Kimura, and Arokiasamy J. Francis. 2006. "Interactions of Rare Earth Elements with Bacteria and Organic Ligands." *Journal of Alloys and Compounds* 408–412: 1334–38. https://doi.org/10.1016/j.jallcom.2005.04.142.

Park, Dan M., Aaron Brewer, David W. Reed, Laura N. Lammers, and Yongqin Jiao. 2017. "Recovery of Rare Earth Elements from Low-Grade Feedstock Leachates Using Engineered Bacteria." *Environmental Science and Technology* 51 (22): 13471–80. https://doi.org/10.1021/acs.est.7b02414.

Park, Dan M., David W. Reed, Mimi C. Yung, Ali Eslamimanesh, Malgorzata M. Lencka, Andrzej Anderko, Yoshiko Fujita, Richard E. Riman, Alexandra Navrotsky, and Yongqin Jiao. 2016. "Bioadsorption of Rare Earth Elements through Cell Surface Display of Lanthanide Binding Tags." *Environmental Science and Technology* 50 (5): 2735–42. https://doi.org/10.1021/acs.est.5b06129.

Sposito, Gary. 2016. "The Chemistry of Soils." *Oxford University Press*, no. Third Edition.

Takahashi, Yoshio, Xavier Châtellier, Keiko H. Hattori, Kenji Kato, and Danielle Fortin. 2005. "Adsorption of Rare Earth Elements onto Bacterial Cell Walls and Its Implication for REE

Sorption onto Natural Microbial Mats." *Chemical Geology* 219 (1–4): 53–67. https://doi.org/10.1016/j.chemgeo.2005.02.009.

Takahashi, Yoshio, Mika Yamamoto, Yuhei Yamamoto, and Kazuya Tanaka. 2010. "EXAFS Study on the Cause of Enrichment of Heavy REEs on Bacterial Cell Surfaces." *Geochimica et Cosmochimica Acta* 74 (19): 5443–62. https://doi.org/10.1016/j.gca.2010.07.001.

Texier, A. C., Y. Andrés, M. Illemassene, and P. Le Cloirec. 2000. "Characterization of Lanthanide Ions Binding Sites in the Cell Wall of Pseudomonas Aeruginosa." *Environmental Science and Technology* 34 (4): 610–15. https://doi.org/10.1021/es990668h.

Tukker, Arnold. 2014. "Rare Earth Elements Supply Restrictions: Market Failures, Not Scarcity, Hamper Their Current Use in High-Tech Applications." *Environmental Science and Technology* 48 (17): 9973–74. https://doi.org/10.1021/es503548f.

Yu, Qiang, and Jeremy B. Fein. 2015. "The Effect of Metal Loading on Cd Adsorption onto Shewanella Oneidensis Bacterial Cell Envelopes: The Role of Sulfhydryl Sites." *Geochimica et Cosmochimica Acta* 167: 1–10. https://doi.org/10.1016/j.gca.2015.06.036.